*Annals of Glaciology*

**Paper**

**Cite this article:** Knight J (2019). Coeval brittle and ductile deformation beneath the late Wisconsinan Puget Lobe, Washington State, USA. *Annals of Glaciology* **60**(80), 100–114. https://doi.org/10.1017/aog.2019.33

Received: 6 June 2019
Revised: 18 September 2019
Accepted: 19 September 2019
First published online: 14 October 2019

**Key words:**
Cordilleran ice sheet; deforming bed; glacitectonics; hydrofracturing; strain

**Author for correspondence**:
Jasper Knight,
E-mail: jasper.knight@wits.ac.za



**cambridge.org/aog**

# Coeval brittle and ductile deformation beneath the late Wisconsinan Puget Lobe, Washington State, USA

Jasper Knight

School of Geography, Archaeology & Environmental Studies, University of the Witwatersrand, Johannesburg 2050, South Africa

## Abstract

Late Wisconsinan glacial sediments, exposed on Whidbey Island and Camano Island, Puget Sound (Washington State, USA), were deposited in a proglacial shallow marine/outwash environment during northward retreat of the Puget Lobe of the Cordilleran ice sheet. Sediments mainly comprise massive and cross-bedded sand and gravels, and rhythmically-bedded clay and silt/fine sand couplets, interbedded with diamictons that were deposited by a range of mass flows of different viscosities. Although sediment stratigraphy and ice advance–retreat patterns are well established for the Puget Lobe, brittle and ductile deformation structures within, and separating, these sediment units are less well understood. These structures record the nature of ice–bed interactions taking place in subglacial and proglacial environments. This study examines evidence for these processes and environments. Key deformation structures identified include open to overturned folds, normal and reverse faults, clastic dikes and hydrofractures and passive-loading structures. Evidence for coeval development of ductile and brittle deformation structures shows the close relationship between porewater changes, sediment rheology and sediment system responses to changes in strain caused by ice–bed interactions.

## Introduction

Subglacial and proglacial processes and environments during ice advance–retreat cycles are commonly reconstructed from different glacitectonic and soft-sediment deformation structures present within subglacial, overridden or bulldozed sediments of different types (e.g. Piotrowski and others, 2006; Lee and Phillips, 2008; Rijsdijk and others, 2010; Phillips and others, 2013a, b, 2018a; Knight, 2015). In addition there are significant feedbacks between substrate properties and overlying ice flow, mediated through the development of glacitectonic structures that give rise to variations in porewater pressure within subglacial and proglacial sediments, and variations in meltwater availability at the ice–bed interface (Boulton and Hindmarsh, 1987; Piotrowski and Kraus, 1997; Denis and others, 2009; Phillips and others, 2018b). These structures, indicative of different subglacial strain regimes and their expression in the proglacial environment, may be partially preserved within the sediment profile, or overprinted by later strain events. Such evidence allows for the history of different phases of strain regime and subglacial conditions to be reconstructed (Hindmarsh, 1997; Piotrowski and others, 2006; Lee and Phillips, 2008; Knight, 2015). While such evidence can be recognised in section and at the microscale, the nature and style of interactions between ice and bed are not known with certainty. This study examines the different sediment types and sedimentary and glacitectonic structures present beneath and in front of the retreating late Wisconsinan Puget Lobe of the Cordilleran ice sheet, in order to interpret the nature of subglacial and proglacial processes and environments. This location provides a good case study of these processes because the ice advance–retreat cycle of this ice lobe is well constrained both in time and space, and sediment sections are well exposed within the Puget Sound region (Fig. 1), discussed below. In detail this study (1) describes the regional glacial context and Puget Lobe dynamics; (2) presents new sedimentological and structural data from coastal exposures on Whidbey Island and Camano Island (Puget Sound), including from a range of deformation structures and (3) discusses this evidence in the context of subglacial processes and ice dynamics.

## Regional glacial history

During the last (late Wisconsinan) glaciation, the Cordilleran ice sheet centred on west coast Canada underwent margin oscillation, mainly through development of valley glacier outlets directed through British Columbia valleys to the west, and by the development of more extensive lobate margins to the south (Fulton, 1991; Easterbrook, 1992, 2003). The Puget Lobe was the most dynamic part of the southern margin of this ice sheet (Thorson, 1980; Easterbrook, 1992) and has been well constrained by dating (Porter and Swanson, 1998) and modelling evidence (Booth, 1986, 1991). The sediment stratigraphy of the Puget Lobe during the last glacier advance–retreat cycle (Fraser Glaciation) is well established, comprising terrestrial ice lobe advance (Vashon Stade) over pre-existing outwash sands and gravels (Quadra Sand), depositing glacial tills (Vashon Drift) and forming drumlins across the Puget Sound region. During

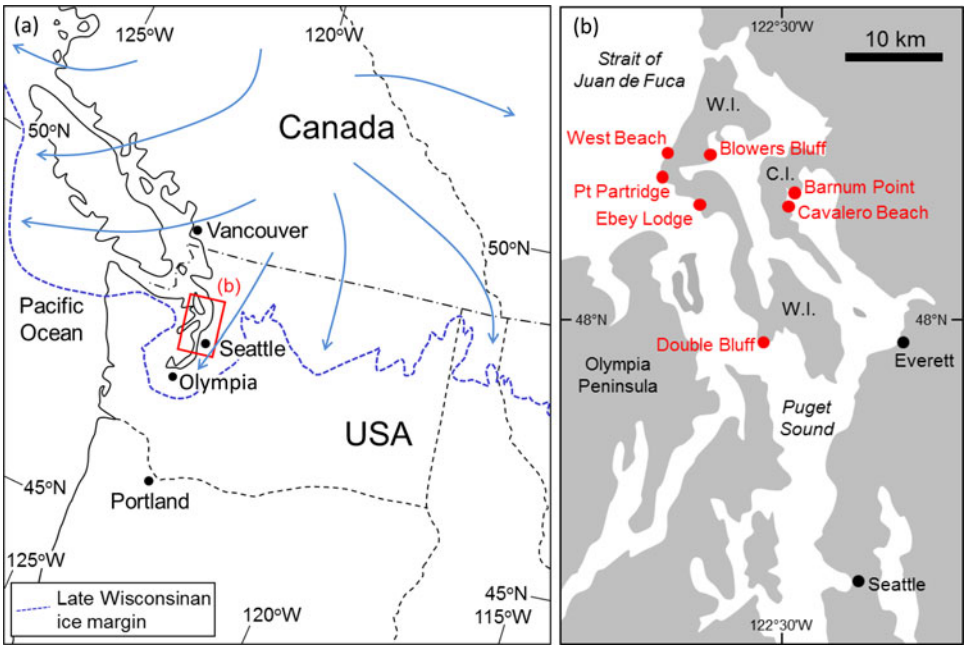


**Fig. 1.** (a) Location of the study area showing the maximal position of the late Wisconsinan ice margin of the Puget Lobe, with LGM ice flow direction marked (blue arrows; after Fulton, 1991) and (b) locations of Whidbey Island (W.I.) and Camano Island (C.I.) within Puget Sound, and the positions of sites named in the text.

the Vashon Stade, advance of the ice lobe incorporated tree wood and shells into the basal till zone, and these have been dated to 14.5–15.0 $^{14}$C ka BP (Hicock and Armstrong, 1985). Deformed and sheared wood along this advance unconformity is easily observed in section. Northward ice margin retreat following the ice lobe's maximal position south of Olympia, Washington State, was driven by rising sea level, leading to glacimarine sedimentation during the Everson Interstade in the period 10.3–13.0 $^{14}$C ka BP (Easterbrook, 1969; Dethier and others, 1995). The wide lateral extent of glacimarine sediments suggests rapid ice retreat during this interstadial (Easterbrook, 1992) but the presence of sorted gravels as lenses within finer glacimarine sands and muds suggests more episodic sedimentation took place in the form of grounding line fans, corresponding to still-stands during ice retreat (Domack, 1984). Recent work by Demet and others (2019) from limited exposures on Whidbey Island suggests grounding line fans prograded in the form of debris flows with rhythmic sedimentation driven by tidal pumping.

While these studies have focused on regional sediment stratigraphy (Fig. 2), there is an absence of discussion on ice–bed interactions during ice advance and in particular during ice retreat phases, based on field observations of deformation structures of different types. This is important in this instance because sea-level oscillation is thought to have controlled accommodation space during ice retreat (Demet and others, 2019) and therefore the degree of ice–bed interactions that can give rise to sediment deformation of different styles. Sea-level oscillation is recorded by the presence of nested relict shorelines up to 88 m asl and planated surfaces are present at different levels across the region (Kovanen and Slaymaker, 2004; Mosher and Hewitt, 2004). Throughout the lobe advance–retreat cycle, including lift-off from the ice bed that triggered net retreat, ice–bed interactions (as recorded by different deformation structures) or their relationships to pinning points during ice retreat or their relationships to regional sediment stratigraphy are not well known. This is the focus of the present study.

## Methods

Sedimentary sections were logged in the field from seven sites on Whidbey Island and Camano Island, Puget Sound, using standard lithostratigraphic codes for glacigenic sediment facies (Eyles and others, 1983). Sites were located with a handheld GPS. These sediments were set in a lithostratigraphic context outlined in previous studies (Easterbrook, 1969, 1992; Hicock and Armstrong, 1985) (Fig. 2). Where present, the strikes of sedimentary and glacitectonic structures were measured using a compass corrected for declination (+15°), and dips where appropriate. Sediments and structures recorded in the field were interpreted with respect to the regional context and relationships between deformation structures and subglacial/proglacial environmental conditions and processes derived from analogues described in the literature. Sites examined in this study and their major sediment properties are listed in Table 1.

## Results

The geomorphology of Puget Sound islands has been well mapped and comprises drumlins and marine-planated surfaces at various levels formed during advance and retreat phases, respectively (Goldstein, 1994; Kovanen and Slaymaker, 2004). Meltwater incision and creation of erosional relief at and in front of the ice margin provided accommodation space for infilling by proglacial (glacifluvial and glacimarine) sediments, commonly located above a regional erosional unconformity (Booth, 1994). Sites examined in this study show several erosional surfaces that fit into this regional context, and different subglacial and proglacial sediment facies including water-sorted sands, gravels and clays/silts (muds) and diamictons formed in subglacial and proglacial settings. The sediment units and deformation structures at seven key sites on Whidbey Island and Camano Island are described from north to south and with reference to regional stratigraphy (Fig. 2), and then interpreted with respect to processes and environments.

### *West Beach*

This site was discussed briefly by Demet and others (2019). Here, a 20 m high exposure comprises 10 m of basal stratified sand (Ss facies; unit 1) with a silty diamicton and stratified sand unit (Dmm and Ss facies; unit 2) above (Fig. 3a). These conformable

https://doi.org/10.1017/aog.2019.33 Published online by Cambridge University Press

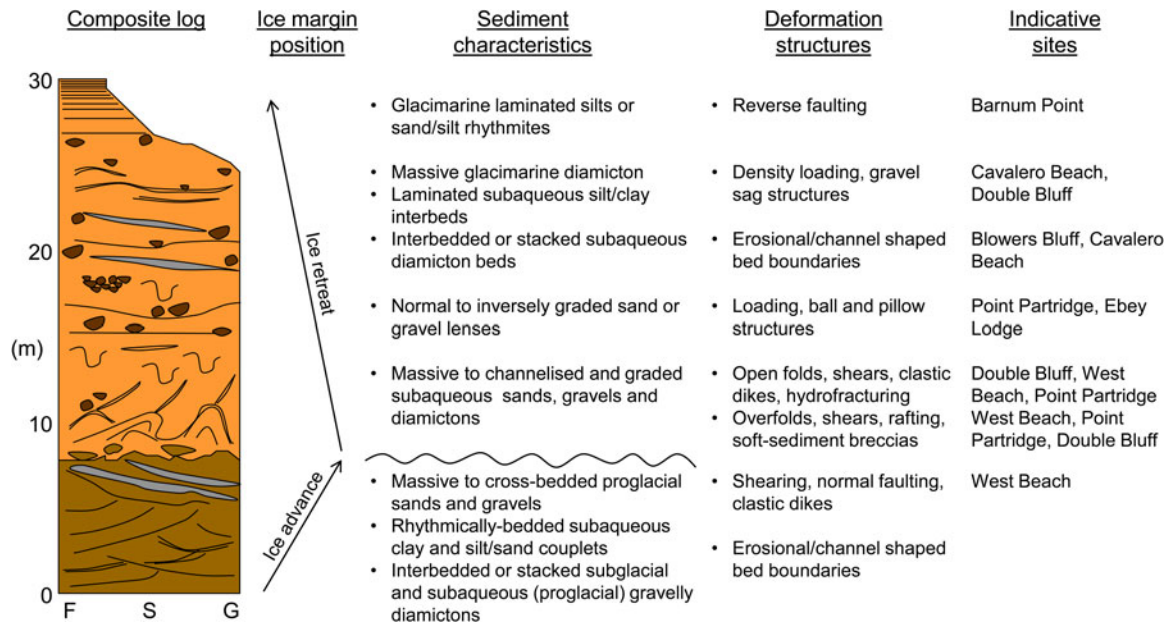


**Fig. 2.** Composite regional stratigraphy of Puget Lobe advance–retreat (after Easterbrook, 1969; Domack, 1984) and stratigraphic positions of typical deformation structures identified at sites discussed in the text. Note that detailed facies logs from individual sites are presented in Figure 3.

**Table 1.** Locations of sites examined in this study and their major sediment properties

| Site | Location | Principal depositional environment |
|---|---|---|
| Camano Island | | |
| Barnum Point | 48°12′36″N, 122° 26′31″W | Subglacial to proglacial |
| Cavalero Beach | 48°10′37″N, 122° 28′44″W | Proglacial, subglacially influenced |
| Whidbey Island | | |
| West Beach | 48°15′28″N, 122° 45′09″W | Ice readvance into marine environment |
| Blowers Bluff | 48°14′36″N, 122° 39′43″W | Proglacial subaqueous outwash |
| Point Partridge | 48°13′44″N, 122° 46′09″W | Subglacial readvance, marine influence |
| Ebey Lodge | 48°11′10″N, 122° 42′05″W | Proglacial, marine influenced |
| Double Bluff | 47°58′22″N, 122° 31′33″W | Proglacial |

units are laterally continuous, tabular and flat lying. Unit 1 comprises broad lenses of massive and well-sorted medium to coarse sand (Sm facies) that are a few m wide and dm-scale in depth. These lenses are separated by cm-scale fine sand and discontinuous clay interbeds, expressed as rhythmites, that are undulating in profile, laterally continuous and occasionally rippled (Figs 4a and b). Thin (cm-scale) but laterally extensive intraformational diamicton beds (Dmm facies) lie conformable to clay bed surfaces (Figs 4d and e). These are clay and silt matrix-dominated with dispersed pebbles (<3 cm diameter). The clay beds (<1 cm thick and 5 m in extent) at the bottom of this unit contain woody debris that has been incorporated into these sediments, especially along bed boundaries (Fig. 4c). Clay beds increase in frequency but maintain a constant thickness upwards. The top of this basal unit comprises a 1 m-thick and laterally continuous, flat-lying and finely laminated clay/silt bed (Fl facies) that has been passively loaded by overlying thicker diamicton beds. The uppermost silty diamicton and stratified sand unit (unit 2, 10 m thick) overlies a laterally extensive, planar and disconformable surface. Tabular and stratified beds of variably sorted medium to coarse sands (Sm and Ss facies) dominate at the base of unit 2. Isolated cobbles to boulders are found occasionally within the sand beds. Thin lenses of intraformational pebbles and cobbles (<3 m lateral extent, 6 cm thickness) become more common upwards and have a British Columbia (northern) provenance. The majority of unit 2 comprises well sorted and tabular beds (2 m thick) of stratified medium sand (Ss and Sm facies) that are arranged into shallow channels with plane-parallel aggradational sand infills. Channel structures are 8–15 m wide and <3 m thick. Channel axial orientation is not well observed. Upsection, diamicton beds (Dmm and Dms facies) become more common and are separated from underlying massive sand beds by erosional unconformities and these become more apparent upwards. No deformation structures are observed along these erosional contacts. Diamicton beds (0.5–1.0 m thick) are laterally continuous, massive and tabular and contain pods and stringers of pebbles to cobbles towards the top of each bed. These clasts (<12 cm diameter) are subrounded to very well rounded granite clasts with a northerly provenance and do not show a dominant orientation, although some larger boulders have an a(t) fabric dipping to 030°. Mud stringers (cm-scale) are also present within and separating the diamicton beds. It is notable that soft-sediment deformation structures, recorded as sags and ball and pillow structures (1.5 m wide, 80 cm high), are developed where alternating diamicton and mud beds are observed (Fig. 4f). Here, the muddy diamicton matrix has held this material intact and larger clasts have not preferentially sagged. At the top of the section, a massive to laminated (Fl facies) silt bed 2–3 m thick unconformably overlies massive sand. The silt bed thickens to the south and is disrupted by conjugate faults that are intersecting and have cm-scale net displacement.

Sediments of unit 1 at West Beach are interpreted to have been deposited in a proglacial and shallowing-up environment, evidenced by rhythmically-bedded sands and silts deposited in a quiet-water laterally extensive basin, interrupted by episodic

https://doi.org/10.1017/aog.2019.33 Published online by Cambridge University Press

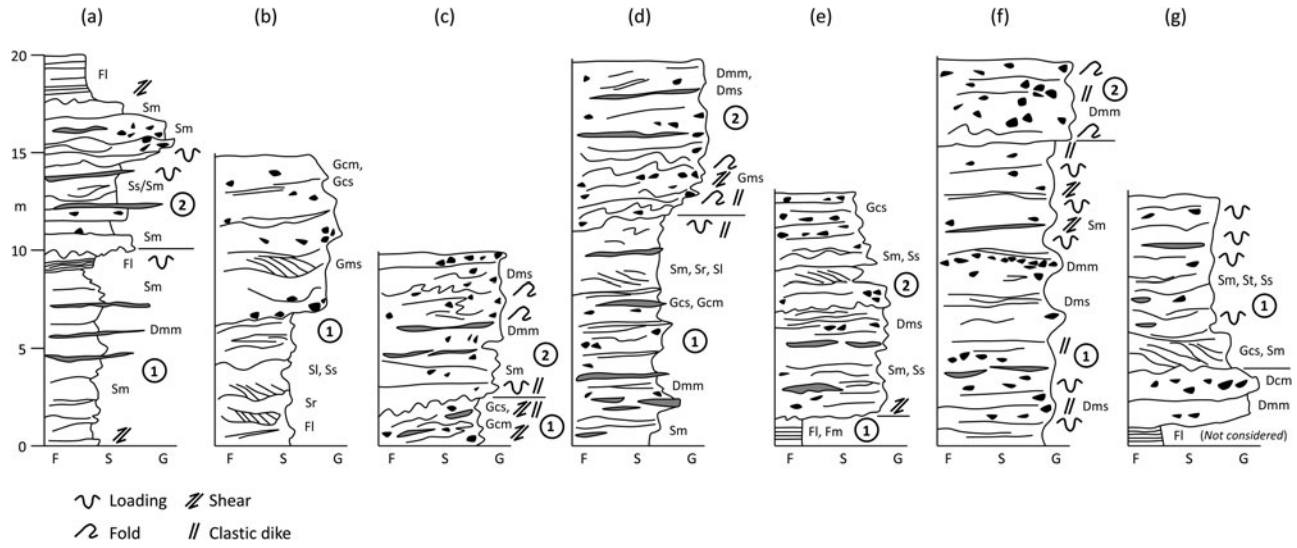


**Fig. 3.** Schematic logs of sediments examined across Whidbey Island and Camano Island, Puget Sound. (a) West Beach, (b) Blowers Bluff, (c) Point Partridge, (d) Barnum Point, (e) Ebey Lodge, (f) Cavalero Beach and (g) Double Bluff. Circled 1, 2 are sediment units discussed in the text.

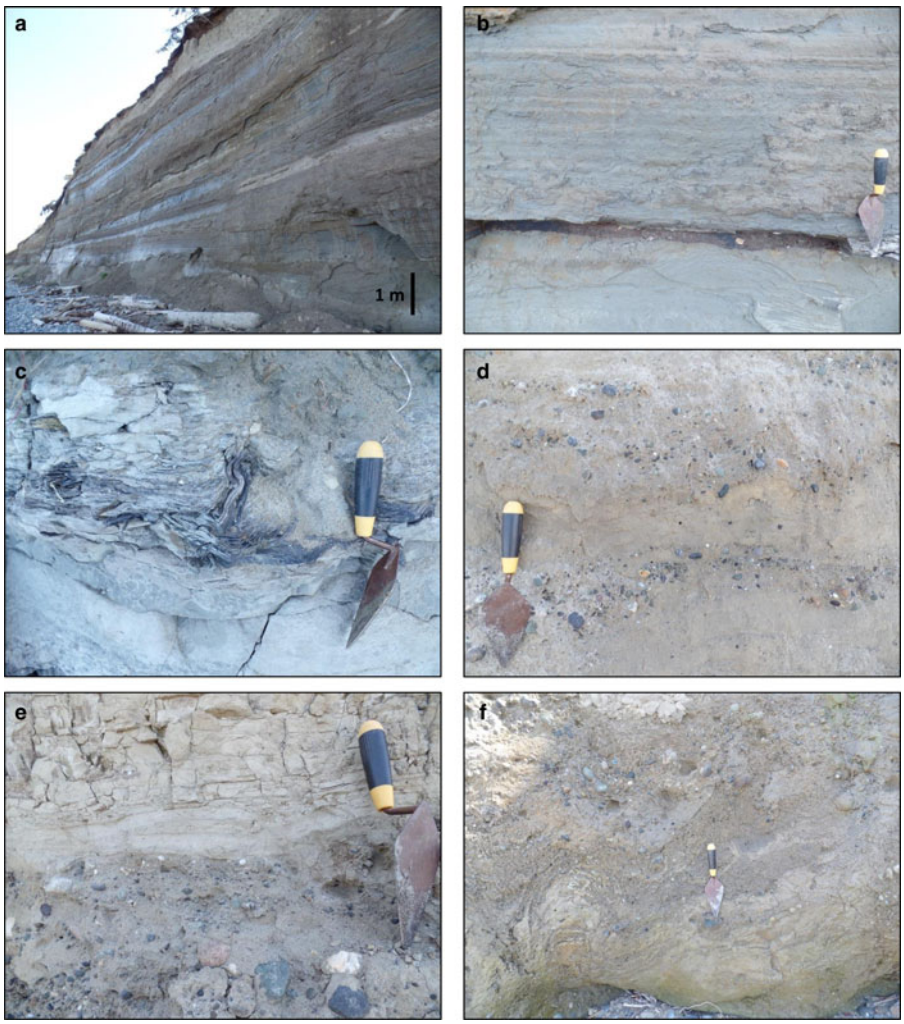


**Fig. 4.** Sediments and deformation structures at West Beach. (a, b) Flat-lying rhythmites of sand and silt/clay separated (at base) by an intraformational debris flow bed above an undulating erosional surface; (c) deformed tree debris incorporated into basal sediments by ice readvance across a vegetated forefield; (d) diffuse sand and diamictic gravel beds exhibiting an undulating morphology; (e) brittle-fractured silt beds overlying fine sand and diamictic gravel beds and (f) ball and pillow structures developed in adjacent silt and gravel beds along with minor brittle fracture and rafting of silt slabs in the lowermost unit (below the trowel). Trowel is 19 cm long.

mass flows (diamicton beds). Sand beds and lenses record more proximal and shallower water environments, likely as a transition to an outwash plain (e.g. Krzyszkowski, 1994). This is evidenced in unit 2 by the presence of shallow and infilled channels typical of an outwash plain environment (Landvik and Mangerud, 1985). The thin and discontinuous mud beds and diamictons that develop upwards in this unit likely reflect higher water availability. This is also shown by the presence of soft-sediment deformation and ball and pillow structures, formed by density contrasts in an environment susceptible to passive loading (Owen and Moretti, 2011). Inferred changes in water availability and/or depth through this section at West Beach may reflect either variations in

https://doi.org/10.1017/aog.2019.33 Published online by Cambridge University Press

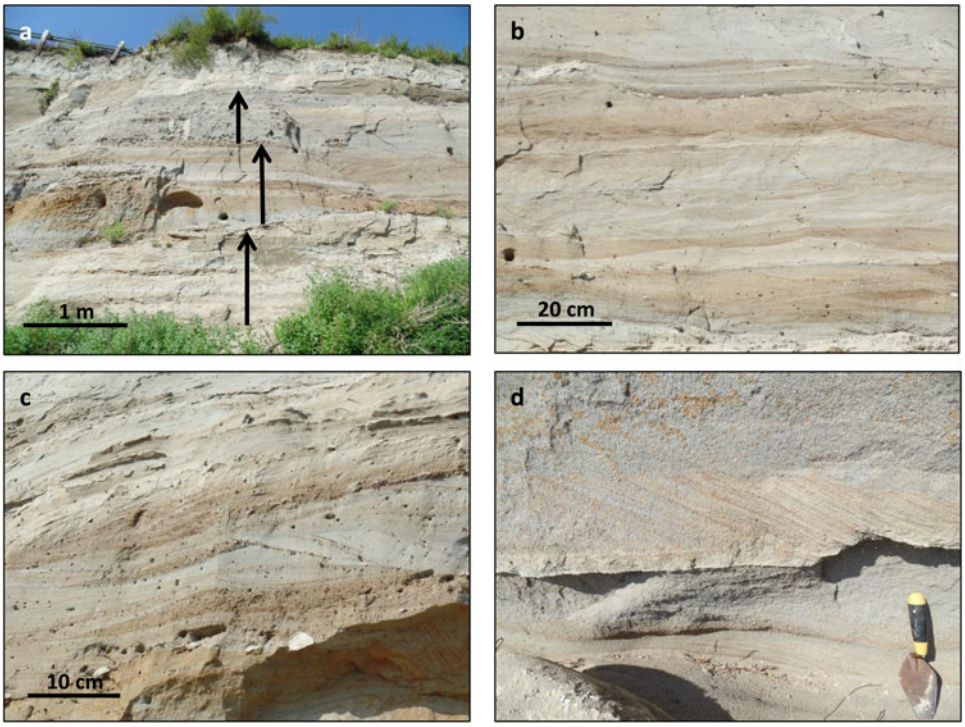


**Fig. 5.** Sediments and deformation structures at Blowers Bluff. (a) Metre-scale sand and silt packages (indicated by the arrows) within cut and fill channels; (b) ripple and trough cross-bedded sands with silt drapes, and mud clasts as lags at the base of channel fills; (c) detail of mud clasts and superimposed multi-storey channel fills with normally graded cm-scale infills or laterally persistent sand laminae and (d) rectilinear cross-bedded surfaces within dm-scale channelised sand packages marked by erosionally unconformable boundaries. Trowel is 19 cm long.

proximity to the ice margin, or changes in accommodation space as a result of sedimentation.

### Blowers Bluff

At this site, mentioned by Easterbrook (1992) and Dethier and other (2008), rhythmically-bedded sands and silts are overlain by massive to cross-bedded sands, occasionally gravels, within a single depositional unit (Figs 3b and 5). Sand and silt beds (Sl, Ss and Fl facies), in total 14 m thick, are laterally continuous and undisturbed but are arranged in distinctive m-scale packages located within broad (10–12 m) and shallow (50–80 cm) multi-storey channels that are separated by planar and undulating erosional unconformities (Fig. 5a). Within these packages, individual beds (4–20 cm thick, <12 m lateral extent) are largely conformable to each other, occasionally with reactivation surfaces (Fig. 5b). These beds comprise planar well-sorted medium to fine sand (Ss, Sl, Sh and Sm facies), trough cross-bedded medium sand (St facies), planar cross-bedded medium to coarse sand (Sp and St facies) and ripple cross-laminated fine sand (Sr facies). The latter shows type B climbing ripple-drift cross-lamination (sensu Jopling and Walker, 1968), rising to the southeast but with high directional variability. This is also shown in the other trough cross-bedded facies: as an example, one cross bed dips 020 to 060°, but this angle flattens along the same bed in the direction of sediment deposition (to the south). The directional signatures of structures within adjacent beds, or between channel fills and the sediments into which the channel is incised, may also vary by about 90°. Soft-sediment intraclasts of massive silt (Fm facies) are also present above bounding contacts at the base of sand beds (Fig. 5c). These clasts (1–4 cm diameter) are dispersed laterally, discontinuous, flat-lying and subrounded in morphology. There is no clear indication of these soft-sediment clasts being broken up during transport. Gravel beds (8 m thick in total) at the top of the Blowers Bluff section are conformable to the underlying sands. Units containing cross beds are laterally continuous and comprise different gravel facies (Gcm, Gcs and Gms) where individual beds are 30–50 cm thick and associated with incised channels that have asymmetric infills, similar to those in the underlying sands. Rafted intraclast blocks of silt (Fm facies) up to 1.2 m long and 50 cm thick are located within the base of the gravel beds.

Sediments at Blowers Bluff record deposition in a proglacial outwash environment, evidenced by the presence of shallow and migrating channels with sand beds and channel infills directed in different directions (Landvik and Mangerud, 1985). The sediment packages located between laterally extensive unconformities may correspond to cycles of sedimentation events, possibly driven by meltwater availability. Such cyclic aggradational episodes have been described from Pleistocene outwash plains (Pisarska-Jamroży and Zieliński, 2014). Cross-bedding of different types reflects infilling episodes within channels in more distal outwash locations (Blažauskas and others, 2007). An upward increase in gravel beds suggests more competent fluvial transport and thus increasing proximity to the ice front. The absence of diamicton interbeds suggests a location far enough away from the ice front to exclude mass flows of different types. Soft-sediment intraclasts within gravel and sand beds indicate substrate erosion during sediment transport, and erosion of more proximal and pre-existing fine sediment beds from the glacier forefield. The relatively intact yet subrounded nature of the intraclasts suggests a relatively short transport distance. Morphologically similar soft-sediment clasts have been reported from other outwash settings, including elsewhere in Puget Sound (Knight, 1999a, 2009).

### Point Partridge

Point Partridge is mentioned by Dethier and others (1995, 2008) as recording ice contact deposits; however Demet and others (2019) described it as a grounding zone affected by different

https://doi.org/10.1017/aog.2019.33 Published online by Cambridge University Press

phases and styles of subglacial and proglacial deformation. The exposed section at Point Partridge is 10 m high and comprises two major units (Fig. 3c). Unit 1 is 2 m thick and contains sand, gravel and clay/silt beds that are interbedded and deformed. The upper surface of unit 1 dips below beach level and is overlain generally conformably by unit 2, diamicton and sand beds. In detail, unit 1 contains an intact lens-shaped raft of massive clay that has thin wisps of granules throughout and scattered rare pebbles (<5 cm diameter). This raft (1.5 m thick, 6 m long) is hosted within massive gravels with a significant silty matrix (thus can be termed a diamictic gravel; Gms and Dms facies). Raft margins are sharp and largely intact. The upper surface of the raft however has been variously plucked and sheared resulting in smaller subangular fragments becoming detached from the main raft body (Fig. 6). Several different deformation styles are found around the raft margins. A wedge-shaped fracture aligned 080–260° developed to 40 cm depth from the surface of the raft is infilled with the hosting gravels (Fig. 6a). Larger clasts are aligned parallel to wedge margins. Elsewhere along the upper raft surface, smaller blocks have become detached along minor shear planes, with the direction of fragment transport towards the south, corresponding to regional ice flow (Figs 6b and c). It is notable that the outer edges of many silt clasts are partly armoured by gravels. Laterally, at the base of the section, interactions between silt and gravel beds are shown by the development of ball and pillow structures (Figs 6e and f). In detail, these structures (~10 cm in width, breadth and height when seen in three dimensions) represent the downward sagging of denser materials from above; it is notable that original laminations in the sagged material are preserved. In places, the intact silt beds have been affected by conjugate fractures, but these do not show a dominant alignment direction. The clay/silt rafts and beds are overlain by gravels (Gcm and Gcs facies).

Beds in the surrounding gravels are broadly parallel to the raft surface; upwards, the angle of gravel bed dip increases and the gravel beds (40 cm thick) become finer, more clearly planar stratified (occasionally normally graded) and with amalgamated undulating silt and sand interbeds. At the contact of the gravel beds with overlying unit 2, different styles of water escape, brecciation and dewatering are seen. Shearing and dewatering structures are present at the tops of individual gravel beds. Clastic dikes associated with hydrofracturing (water escape) through interbedded sand and gravel beds are vertically aligned and are located at the top of unit 1. One significant clastic dike is >2 m high and 10–60 cm wide, cuts across the sediment stratigraphy and is associated with both normal and reverse faulting on either side of the dike. There is a planar erosional contact to unit 2. This unit (8 m thick) comprises laterally extensive and massive gravelly diamictons (Dms and Dmm facies) that are interbedded with discontinuous massive sand lenses (Sm facies). These beds (0.8–1.5 m thick) have dispersed subrounded pebbles to cobbles, occasionally arranged into flat-lying single layers. The dominant matrix is medium to coarse sand. Upwards, gravel beds have been affected by folding with consistent axial plane orientation (Fig. 7). Folds are located within single beds and extend laterally over about 5 m, comprising several open and asymmetrical fold elements. Upwards, fold deformations are accommodated within the sediment pile.

Sediments at Point Partridge record processes associated with ice advance or oscillation into a water-dominated (likely glacimarine) environment. Evidence for this is the formation, transport and partial breakage of the clay/silt raft hosted within gravel beds. The presence of dropstones within the clay/silt sediments suggests it was deposited in a glacimarine environment ahead of the ice margin and subsequently overridden. Rafting is most commonly associated with subglacial sediment freeze-on or shearing, and deposition at the ice margin (Croot, 1987). Key to this interpretation is the presence of hosting gravels, interpreted as prograding delta deposits (supporting the viewpoint of Demet and others (2019) as a grounding zone) that increase in depositional angle over time and during southward progradation. Thus, the clay/silt raft is interpreted as deposited at a grounding zone from subglacial transport, and subsequently modified by basal shearing during marginal ice oscillation. Evidence for this is the presence of brittle fracture and shearing features on the raft surface (Figs 6a–d) and ductile deformation features observed more distally and showing the interactions between sediments of different densities (Figs 6e–j). These different structures also reflect changes in properties of the clay/silt sediments: soft-sediment features at raft and sediment margins are indicative of deformation taking place while the sediments were in a softened state. This was followed by postdepositional overconsolidation on the upper raft surface, leading to a more brittle style of deformation by shearing and fracturing, including the fluid injection of gravels along sheared partings as porewater was expelled from the main sediment body. It is notable that this site at Point Partridge is located very near (400 m) to the kettle hole of Lake Pondilla and thus may have been potentially affected by the loss of lateral support, giving rise to faulting.

### Barnum Point

Sediments here (<20 m thick) are organised into two lithostratigraphic units (Fig. 3d) that are tabular in geometry and laterally extensive, with the coastal cliff exposure extending for hundreds of metres. Unit 1 becomes stratigraphically lower laterally, and unit 2 reaches beach level. The basal unit (unit 1, 12–20 m thickness in total) comprises laterally continuous, tabular sand and gravel beds (Sm, Sr, Sl and Gcs facies), individually 20–80 cm thick, that are interbedded with lenses and stringers of diamictons (Dmm facies). In detail, the sand beds are arranged into elongate and undulating lenses with a wavelength of 3–6 m and relief of 50 cm. Beds are composed of poorly sorted medium to coarse sand, and bed boundaries are marked by minor erosional unconformities with granule to pebble lags. Sand beds <10 cm thick form shallow to swaley low-angle sheets that are laterally extensive and do not appear to show a preferred dip direction. The dip angle can vary laterally within individual sand beds. Interbeds of granules to pebbles <4 cm in diameter (Gcs and Gms facies) form discontinuous sheets 8–10 cm thick that pinch out laterally. The base of these interbeds is planar and without significant basal erosion.

These sands and gravels are overlain conformably by unit 2, comprising massive to stratified diamictons (8 m thick in total) interbedded with discontinuous layers and lenses (<2 m long) of massive to cross bedded sands (Fig. 8). The diamicton beds (Dms and Dmm facies) are generally planar, 1.5 m thick with gradational upper and lower boundaries. The diamicton matrix is composed of massive silt to fine sand with dispersed subrounded pebbles <8 cm in diameter. Some diamicton beds contain variously swaley to undulating flow noses defined by changes in clast concentration. This unit also has sand and laminated silt stringers present throughout. These are <1 cm thick and have sharp lower and diffuse upper contacts.

Various deformation structures are observed within unit 2 (Fig. 8). Folds are present within diamicton beds, in particular near the contact between units 1 and 2 and where associated with lenses of laminated fine sands to clays, some of which are overfolded or contorted, especially at the base. Folds vary from symmetrical to asymmetrical, recumbent and sheath. Where asymmetrical, the fold axis verges in a down-ice direction, resulting in an up-ice dipping axial surface. Commonly, individual

https://doi.org/10.1017/aog.2019.33 Published online by Cambridge University Press


**Fig. 6.** Sediments and deformation structures at Point Partridge. (a–d) Evidence for brittle fracture of thick and massive silt bed overlain by gravels and sands: (a) flexural fracture of the silt bed and infilling of gravels from above; (b) U-shaped erosional channel infilled with poorly sorted gravels and angular silt soft-sediment clasts. Note the arc-like erosional surface across the top of the U-shaped channel; (c) fractured and laterally transported silt raft, incorporated into the gravel debris flow; (d) dm-scale silt raft transported by rafting at the top of the underlying gravel flow, supported by high-dispersive pressure; (e–j) evidence for ductile deformation within the silt bed: (e) ball and pillow structure developed in cm-scale silt and sand beds; (f) pods of sand rolled into surrounding silts as the core of a sheath fold; (g) massive gravels deforming into a pre-existing fold developed in the massive silt bed; (h) rounded silt soft-sediment clasts incorporated into a folded silt and sand structure; (i) a silt mega-raft (right) incorporated within a gravel bed. The raft is (d) is located in the top left; (j) complex disharmonic folding in vertically-rotated cm-scale silt beds (left of the trowel), with silt brecciation and sand gravel sags. Trowel is 19 cm long.

folds are developed within the same stratigraphic horizon, and are thus considered to be laterally connected. Repeated folds within the same unit are <1.5 m high, 4 m long and have a variable wavelength of 2–10 m. The largest folds are asymmetrical, occasionally sheath folded and have a closer spacing, whereas more subdued folds are farther apart. The entire lowermost 4.5 m of the section is disturbed by folding within diamicton beds, with settling of heavier clasts into syn-fold hollows, and passive deformation of denser diamicton into less dense materials.

Shearing and hydrofracturing within the diamicton beds is well preserved. Different fault activity relates to ice push followed by sediment relaxation. Shears are listric originating from near

https://doi.org/10.1017/aog.2019.33 Published online by Cambridge University Press

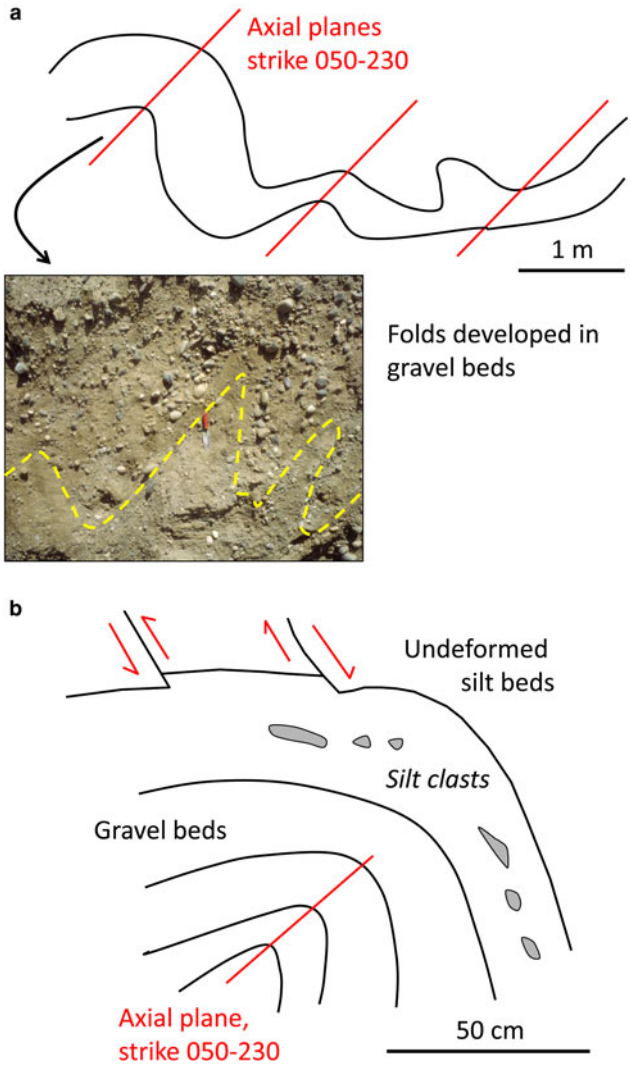


**Fig. 7.** Sketches of folds developed in diamictic gravel beds at Point Partridge. (a) Open and chevron folds with consistent axial plane strikes and (b) interactions between adjacent gravelly diamicton and silt beds when folded. Minor normal faulting of silt beds may reflect bed extension across the top of the fold.

bed bases, and have an up-ice dip. Clastic dikes (cm-scale in thickness but 2–5 m long) are developed in association with some of these shears (Figs 8c–e). All of the clastic dikes observed at Barnum Point have a similar geometry, comprising angular, inclined and planar structures 0.5–2.0 cm wide with sharp and planar margins, and infilled with sorted medium to coarse sand. The grain size of the infill decreases upwards. In places, the clastic dikes rise in a down-ice direction and have a zigzag outline shape in which the dikes appear to have developed along a step-like pattern of brittle fractures, resulting in a pull-apart expression of adjacent sides of the fracture, with a consistent spacing of 3–5 mm. Other structures have a more triangular shape, tapering upwards and are infilled by pebbles and granules derived from underlying sediments (Figs 8b–d). Different dikes are variously cut out by or sometimes penetrate through overlying diamicton beds. Several examples are also observed of clastic dikes that are directed upwards from fold hinges. Figure 9 plots the strikes and dips of different sedimentation and deformation structures within unit 2 at Barnum Point. It is notable that these span a range of alignments, are in most cases vertical structures, and that fold axes are not concordant with southward regional ice flow. Field observations show however that fold properties such as direction of vergence are similar within a single bed but vary between beds. A maximum of 12 folds was counted within a single bed over a distance of about 40 m. These characteristics suggest that deformation structures within single beds are likely genetically related and correspond to the same event.

The sand and gravel beds of unit 1 are interpreted as deposited in a subaqueous proglacial environment, in which tabular and usually massive beds reflect high-sediment supply (Landvik and Mangerud, 1985). The general absence of significant erosion at bed bases suggests a location not close to the ice margin and thus less affected by high-magnitude flood events. Some sand beds containing shallow-angle cross-beds can be interpreted as migrating bars, typical of a proglacial forefield (Blažauskas and others, 2007). The gravelly interbeds located between sand beds are interpreted as unchannelised sheetflows and associated with episodic higher-magnitude flow events. The diamicton beds of unit 2 are interpreted as deposited by debris flows based on their massive texture, presence of dispersed clasts except in association with flow noses where they exhibit inverse grading, gradational bed boundaries indicative of repeated instability and high-depositional water content (as evidenced by passive loading at the base). The deformation structures within unit 2 are associated with changes in porewater pressure as the ice margin became more proximal to this location, giving rise to interactions between ice and bed. The subhorizontal dewatering structures present at the base of the section may reflect porewater escaping from one bed into the overlying bed, in response to sediment deposition and thus loading, also evidenced by the loading structures observed at bed bases (Fig. 8f). In many places, the synsedimentary folding and brittle hydrofractures and fluid flow along developing shear planes appear to be genetically associated. Folding (compression) in both subglacial and proglacial contexts increases porewater pressure directed ahead of the ice margin and facilitates porewater expulsion through the sediment pile. The coincidence of basal parts of clastic dike-filled shear planes with the uppermost hinge plane of folds suggests that this part of the fold is particularly susceptible to thinning and/or fracturing, forming a weak spot for porewater to escape. Thus, based on the co-dependence of these structures on fold formation, they can be termed *parasitic clastic dikes*. It is also notable that overfolding has taken place in immediate association with a shear plane (Fig. 8e), suggesting that differential movement imposed by ice-push (creating the shear plane) then caused folding of the overlying soft sediments. This shear was then exploited as a conduit for fluid migration, creating the clastic dike infill. Oscillation into or minor overriding of these proglacial sediment, in a waterlain environment, means that sediments were successively exposed to ice advance (folding), retreat and relaxation (reverse faulting) phases (e.g. Fig. 8a). Thus their deformation structures can be considered as possibly composite, reflecting several porewater and strain phases.

### Ebey Lodge

This exposure (12 m high) is located within a moraine ridge and shows (unit 1) a basal 1.5 m thick unit of brecciated massive to laminated silty clay (Fl and Fm facies) overlain conformably by (unit 2) sands (Sm and Ss facies) with gravelly diamicton interbeds (Dms facies) (Fig. 3e). The silt beds of unit 1 show mm-scale rhythmically laminated silt–clay sediment packages, separated by more massive cm-scale silts. These beds are parallel, flat-lying, conformable and are not disturbed by ripples, reactivation surfaces or any other structures. However, the uppermost 50 cm of this unit shows intersecting normal and reverse faults that exhibit net movement (compression) in the direction of regional ice flow, to the south, giving rise to lateral offsets of 2–12 cm (Fig. 10a). The contact between units 1 and 2 is generally sharp but jagged, reflecting the partial breakup of the brecciated silts below. These

https://doi.org/10.1017/aog.2019.33 Published online by Cambridge University Press

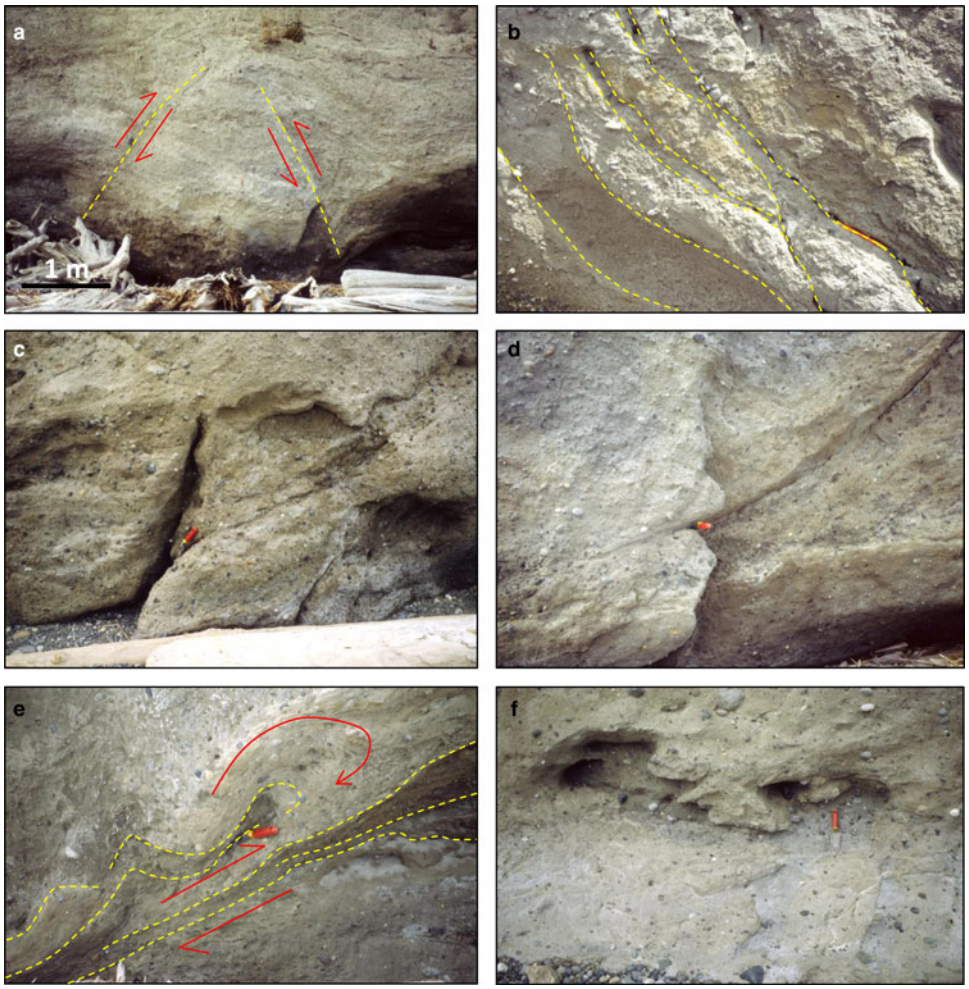


**Fig. 8.** Sediments and deformation structures within unit 2 at Barnum Point. (a) Reverse-faulted margin showing a m-scale downthrown block (relative movement direction indicated); (b) imbricated and stacked diamicton beds (sheared boundaries indicated); (c) upward going m-scale intersecting shears and clastic dikes, at the position of the trowel, with density-drive sags in diamicton beds seen in the top right; (d) thin and linear sandy parting along a listric shear, at the position of the trowel; (e) relationships between shearing and folding structures, outlined in yellow, with direction of relative movement shown by the arrows. The trowel is located in the core of an overturned fold developed in a diamicton bed; (f) density-driven sags developed in diamicton beds that may have been glacitectonically transported. Trowel is 17 cm long, pencil is 15 cm long.

silts are not incorporated into the overlying sediment beds. Unit 2 (<12 m thick in total) dominantly comprises diamicton beds that vary in thickness and properties laterally, and that are interbedded with sand and gravel beds. Individual diamicton beds are 0.4–2.5 m thick, and generally tabular with planar, amalgamated contacts. The diamicton beds become better stratified upwards with a concentration of clasts towards the bottom of individual beds. The sand interbeds are laterally continuous lenses (<6 m in width, 40 cm thick) of well sorted massive sand. Individual lenses (Sm facies) are planar to slightly undulating, located between adjacent diamicton beds, and have erosional lower and amalgamated upper contacts. More laterally extensive and tabular sand beds (Ss facies, 50–80 cm thick) are cross-bedded with planar erosional lower and undulating upper contacts. Gravel interbeds (Gcs facies) are 1.5–2.0 m thick and wedge out laterally, associated with erosional upper contacts. The gravels are clast supported by subrounded to well-rounded pebbles (<7 cm diameter). The diamicton beds, dominant in unit 2, are massive to poorly stratified (Dmm and Dms facies), varying in medium to coarse sand matrix content such that some patches of poorly sorted gravel (Gcm and Gcs facies) are present. Subrounded pebbles and cobbles (<12 cm diameter) within these beds are dispersed throughout. Sand stringers and clast-supported pebble lenses are common (Figs 10b and c).

Sediments at Ebey Lodge were deposited in an ice-marginal environment, evidenced by location of the section within a moraine ridge that clearly extends across Whidbey Island (e.g. Demet and others, 2019). The silty beds of unit 1 are interpreted as waterlain sediments deposited in a quiet-water environment. The presence of rhythmically-laminated packages unaffected by any water disturbance suggests a proglacial lake setting (Shaw, 1975) but a marine setting would fit with regional evidence (Demet and others, 2019). The faulting in the upper part of the profile reflects subsequent ice overriding (either at this site or more up-ice), likely associated with building of the moraine ridge. Deposition of the overlying sands, gravels and gravelly diamictons suggests a water-influenced environment, evidenced by the interbedding between better sorted sands and gravels, and more poorly sorted diamictons deposited by mass flows consistent with an increase in local relief caused by moraine ridge formation (van der Wateren, 1994). The presence of cross-bedding within the sand beds suggests nonconstrained underflows took place within a lake or marine environment.

### *Cavalero Beach*

This section is 200 m long and <20 m high (Fig. 3f) and comprises two sediment units dominated by diamicton beds containing laminated silt/clay interbeds. In unit 1 (16 m thick in total), the diamicton beds (Dmm and Dms facies) are laterally continuous, vary in thickness (0.3–1 m thick) and are inclined (<8° to

https://doi.org/10.1017/aog.2019.33 Published online by Cambridge University Press

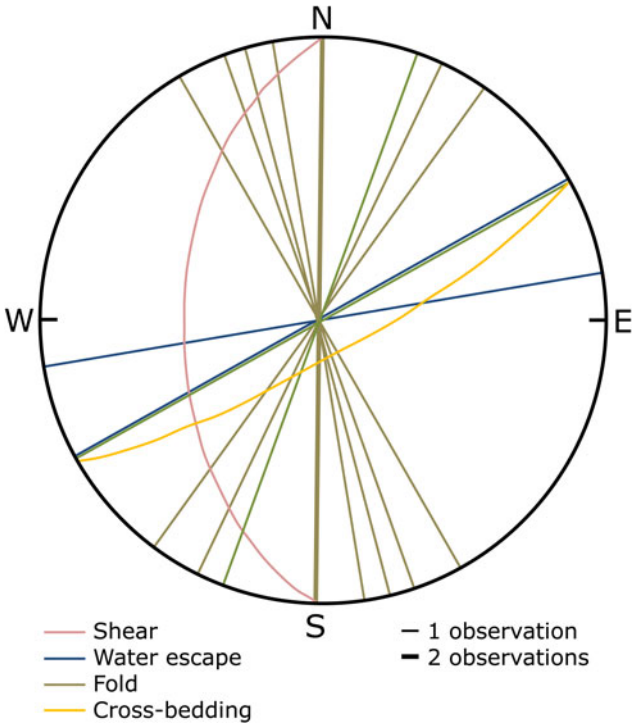


**Fig. 9.** Lower hemisphere stereoplot of various depositional and deformational structures within unit 2 at Barnum Point.

south) to flat lying. Both bed thickness and dip angle decrease southwards. Individual beds terminate laterally in a rounded zone marked by a higher concentration of clasts (Fig. 11). Diamicton beds are matrix dominant (80–90%), comprising medium to coarse sand with subrounded to well-rounded granite and quartzite pebbles (<10 cm diameter) that are dispersed throughout the bed, occasionally with subrounded boulders <50 cm diameter. Clasts are striated and bullet-shaped. To the south, clasts become more common and concentrated at the top of the bed and with a(p) fabrics, but there is no accompanying variability in the matrix component. Some m-scale granite erratics released by coastal erosion from these beds are found as boulders on the adjacent beach. The diamictons within unit 1 also contain gravel-dominated sag structures located within the middle of some individual beds. These structures (<1 m wide, 30 cm deep) are symmetrical and tear-drop shaped and contain clast-supported clusters of pebbles (<6 cm diameter) within the middle of the sag. Individual sag structures are not connected to each other laterally and do not show any particular spatial or stratigraphic patterns. Unit 2 (4–6 m thick in total) comprises a massive diamicton (Dmm facies) that overlies a laterally continuous and flat-lying erosional contact. Texturally, there is no distinction between the upper and lower diamictons, but the upper one contains overfolds that are preferentially developed in clast-poor layers, folded around less mobile clast-rich layers. Within both diamicton units, individual beds are commonly separated by thin and laminated silt/clay interbeds (Fl facies) that are <8 m long and <10 cm thick. The laminae are planar and undisturbed although in some places small (<1 cm) rounded clasts are present, dispersed throughout. The interbeds pinch out laterally and may be deformed by loading from overlying beds, or cm-scale brittle fractures within upper parts of the interbeds that have internally displaced laminae by a few mm to the southeast.

Within both depositional units, a range of deformation structures is present, in particular towards the tops of individual beds. In the silt/clay interbeds, shears can be identified, forming slickensides along lamina partings. Clastic dikes are present at the tops or bottoms of individual beds. These are subvertical and linear structures, 0.2 to 3 m long and 1 to 25 cm wide, with diffuse upper and lower ends but well-marked middle sections defined by sharp and planar fractures between which sediment has been injected (Fig. 11). This internal sediment is texturally similar to, or slightly finer than, the host diamicton but clasts are absent. Dike margin strike is generally 060–240°.

The diamicton beds at Cavalero Beach are interpreted as debris flows, directed away from the ice margin and in a waterlain environment (van der Wateren, 1994). This environmental setting is evidenced by the dispersed clasts within the diamicton beds; the presence of sag structures indicative of clast floundering within water-saturated sediments; and laminated clay interbeds separating individual diamicton beds and that contain dropstones. The diamictons are interpreted as debris flows generated down shallow subaqueous slopes. Laterally, the diamicton beds show some evidence of internal sorting during transport, in which clasts with a(p) fabrics have been surfed on flow tops, maintained by high-dispersive pressure (Mulder and Alexander, 2001). The association of clastic dikes at tops and bottoms of these beds is likely due to loading at the bottom of the beds, and then brittle fracture associated with upward porewater expulsion as clasts settle within the flow. Flow collapse and compaction took place near the flow nose as a consequence of porewater expulsion, resulting in rapid velocity decrease and flow nose 'freezing'. This is evidenced by the rounded front of the flow, indicative of a loss of porewater, rather than a long and thinning runout zone indicative of coarse sediment loss behind the flow nose (Talling and others, 2012). The laminated interbeds are interpreted as periods of sediment rainout through the water column following the passage of turbulent debris flows.

### Double Bluff

This site was mentioned by Dethier and others (2008). Here, a section 12 m high contains massive silts overlain by a massive matrix dominant diamicton and then a gravelly diamicton. Easterbrook (1992) considered these to belong to the penultimate glaciation on the basis of constraining amino acid ratios from overlying glacimarine sediments. These basal sediments are thus not considered further here. However, the gravelly diamicton is in turn overlain by a single sediment unit (8 m thick in total) comprising massive to stratified well-sorted sands (Sm, Ss and St facies; 1.5–4.0 m bed thickness) infilling low points on the diamicton surface (Fig. 3g). These beds are arranged within broad, multistorey and cross-cutting channels and contain single gravel or silt interbeds located above erosional unconformities. Isolated pebbles (<6 cm diameter) are dispersed throughout the cross-bedded units.

Laterally, the basal facies of this unit comprises 4 m of granules with laterally continuous dm-scale stratification and coarse sand to pebble interbeds, some of which are cross-bedded (Gcs and Ss facies). These include cross-bedded and cut and fill sands grading up to fine sand and silt beds with ball and pillow structures. These sediments are overlain unconformably by flat lying massive to rippled medium sand (Sm and Sr facies) with vertically aligned ball and pillow structures <1.5 m high, 2 m wide and with a wavelength of 1 m. These structures are developed in the massive sand beds and are identified based on their being slightly coarser than the surrounding sediments. Sand beds are disturbed in different ways. Beds may be disturbed along vertically aligned faults or upward-going dewatering structures present in the bottom parts of individual beds. There is no lateral displacement recorded on adjacent sides of these structures. Larger-scale bed disturbance is also shown in the upper 4 m of the profile. Here, basal liquefaction of fine sand beds resulted in the mixing of these sediments

https://doi.org/10.1017/aog.2019.33 Published online by Cambridge University Press

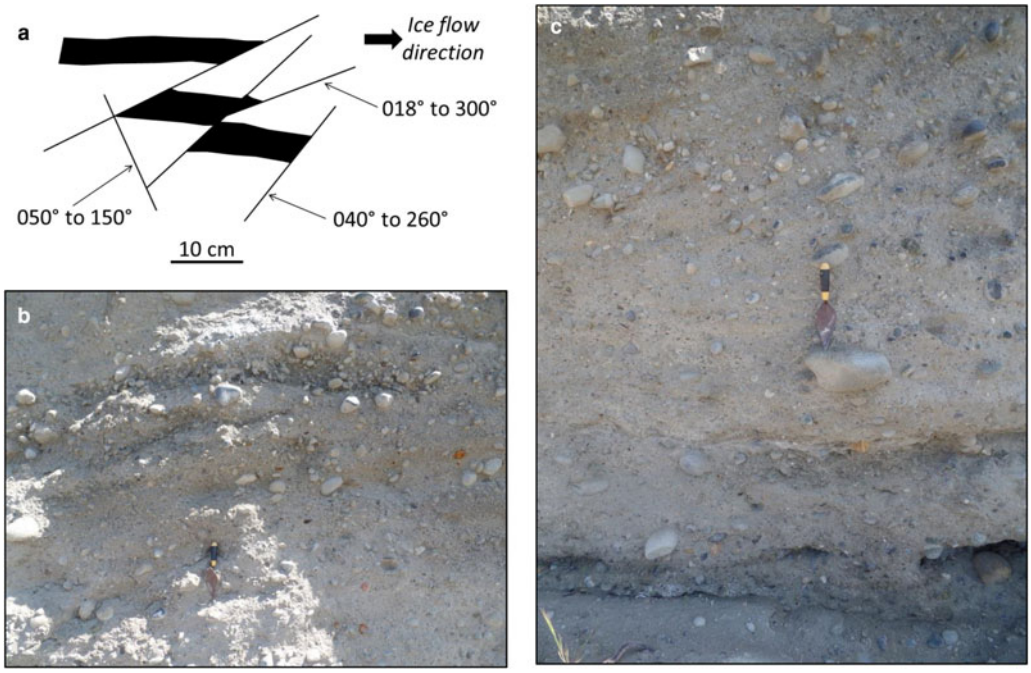


**Fig. 10.** Sediments and deformation structures at Ebey Lodge. (a) Sketch of inclined faults and deformed mud beds (black shading), showing the dip direction and dip angle; (b) inversely bedded gravel lenses separating diamicton beds and (c) deformed mud beds at the base of inclined diamictic debris flows. Trowel is 19 cm long.

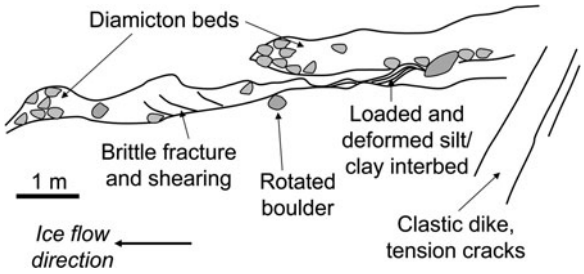


**Fig. 11.** Sketch of different deformation structures present within unit 1 at Cavalero Beach.

with overlying coarser sands, and the injection of sediment, in a down-ice direction, along pre-existing bed partings (Fig. 12). Pre-existing bedding structures have been deformed vertically, forming dm-scale ball and pillow and diapiric structures within the fluidisation zone.

The sand beds at Double Bluff reflect deposition in a proglacial water-influenced environment, evidenced by the presence of water-sorted and cross-bedded sediments within channels incised into an outwash plain (Salamon, 2009). Deposition took place in a proglacial environment in which large-scale channels were migrating across an extensive and uniform outwash plain (Blažauskas and others, 2007). This is evidenced by the general absence of gravel beds or lags within incised channels, or any transported soft sediment clasts. The deformation structures within the sand beds at Double Bluff reflect rapid porewater movement through the sediment pile. Upward-directed movement is suggested by an upward decrease in degree of sediment mixing (fluidisation) and narrowing of the structural expression of this porewater flow, through development of hydrofractures that thin and pinch-out upwards (Lowe, 1975; Phillips and others, 2007). This reflects an upward decrease in water pressure and the accommodation of liquefied fine sands within the overlying undisturbed sand. The absence of any lateral displacement associated with the sediment injection structures suggests that this was not affected by either ice-push or the generation of faults within the sand beds. The presence of upward-going sediment injection structures, however, suggests steep proglacial hydraulic gradients, possible controlled by permafrost aquicludes that can act to focus groundwater movement ahead of the ice margin and allow porewater to burst through overlying sediments causing large-scale fluidisation (Boulton and Caban, 1995). This process has been reported from proglacial forefields (Knight, 2006).

## Discussion

Sediments and sedimentary structures on Whidbey Island and Camano Island reveal the nature of glacier–substrate dynamics and processes during the last ice lobe advance–retreat cycle. In detail, the presence of diamicton interbeds throughout both subglacial and proglacial parts of the stratigraphy (e.g. West Beach, Barnum Point, Ebey Lodge and Cavalero Beach) shows that there were repeated episodes of sediment instability, driven by different styles of ice–bed/sediment interactions (e.g. Phillips and others, 2013b). These include (1) subglacial recoupling and development of the deforming layer behind the ice margin; (2) recoupling at the marine grounding line and triggering of glacimarine mass flows; (3) glacitectonic shearing, sediment detachment and rafting and (4) pervasive ductile sediment deformation and folding below and at the front of the ice margin. There were also indirect effects of ice–bed interactions, seen through changes in porewater pressure leading to hydrofracturing (clastic dikes) and fluidisation (ball and pillows, density settling) (e.g. Dreimanis and Rappol, 1997; Phillips and others, 2007; van der Meer and others, 2009). Such effects are seen at Point Partridge, Barnum Point and Double Bluff.

Table 2 summarises the range of evidence in the Puget Sound area for different styles of deformation. The fact that retreat of the Puget Lobe took place rapidly and dominantly at a marine or tidewater margin (Easterbrook, 1969) means that deformation was likely driven by variations in ice–bed coupling – potentially caused by tidal flexure and thus ice lift-off and recoupling – and not by variations in subglacial thermal regime. However,

https://doi.org/10.1017/aog.2019.33 Published online by Cambridge University Press

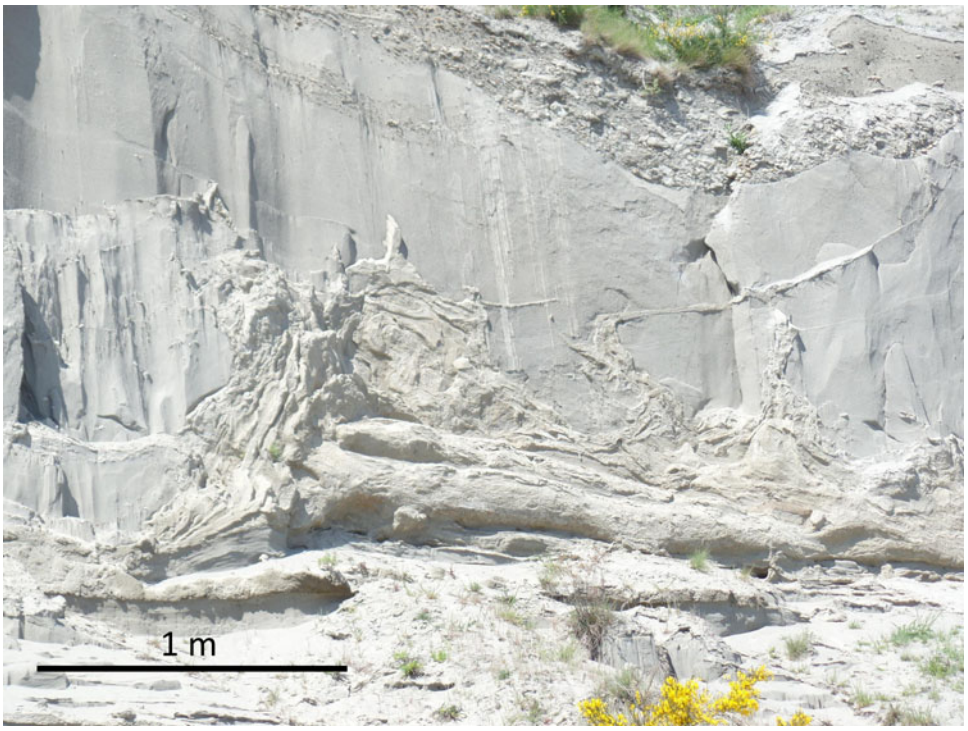


**Fig. 12.** Upward-directed movement of fine sediments leading to bed deformation and parasitic clastic dikes at Double Bluff.

**Table 2.** Evidence for different deformation styles at the sites discussed in this study

| Deformation style | Evidence | Sites where observed |
|---|---|---|
| Ductile deformation | | |
| Undulating bed surfaces | Density-driven soft-sediment deformation | West Beach, Ebey Lodge |
| Open folds, overfolds | Ice overriding, sediment drag-folding both subglacially and where water-saturated muds are affected by the passage of overlying fluidal mass flows | West Beach, Point Partridge, Barnum Point |
| Gravel/sand lobes, ball and pillow structures | Density-driven sinking | Point Partridge, Barnum Point, Cavalero Beach |
| Brittle deformation | | |
| Planar and zigzag-form clastic dikes | Water escape associated with glacial hydrofracturing | Barnum Point |
| Upward- and downward-going clastic wedges | Water escape structures driven by porewater over-pressurisation caused by loading | Point Partridge, Barnum Point, Double Bluff, Cavalero Beach |
| Breccias and sediment rafts, soft-sediment clasts | Glacial hydrofracturing, bedload transport within proglacial channels, rafting supported by dispersive pressure within fluidal flows | Blowers Bluff, Point Partridge, Cavalero Beach |
| Normal/reverse faults | Post-dilatant collapse, meltout of buried ice | Barnum Point, Ebey Lodge |
| Shear planes | Ice–bed coupling and shearing within subglacial sediments; thin clastic dikes connecting basal shears correspond to hydrofracturing and water escape during ice–bed coupling | Barnum Point |

sediments of different types have different geotechnical properties related to their grain size and permeability, and these properties control porewater pressure variations and thus water migration through the sediment pile (Lee and Phillips, 2013). Ductile deformation styles reflect active interactions between ice and bed (folding) and passive responses within the sediment pile (gravity sags). Structural evidence for the consistency of open-fold axes at Point Partridge (Fig. 7) shows that these folds were formed by ice push. Other overturned or disharmonic folds at West Beach (Fig. 4) and Barnum Point (Fig. 8) were formed as a consequence of porewater migration and fluidisation leading to structural collapse (e.g. Owen and Moretti, 2011). The trigger for this may have been increased porewater pressure within subglacial or immediately-proglacial sediments caused by ice advance or ice–bed recoupling. Brittle deformation styles (Table 2) including the development of clastic dikes at Barnum Point (Fig. 8) and Cavalero Beach (Fig. 11) are also related to increased porewater pressure, leading to sediment fracturing and then fluidal transport of fine sediments through the fracture zone. At Barnum Point, both fractures (forming imbricate slabs; Fig. 8b) and upward-going clastic dikes are seen. Hydrofracturing and the formation of upward-directed clastic dikes have also been noted from this region by Huntley and Broster (1993). Most commonly, such features are reported from the subglacial environment inside the ice

https://doi.org/10.1017/aog.2019.33 Published online by Cambridge University Press

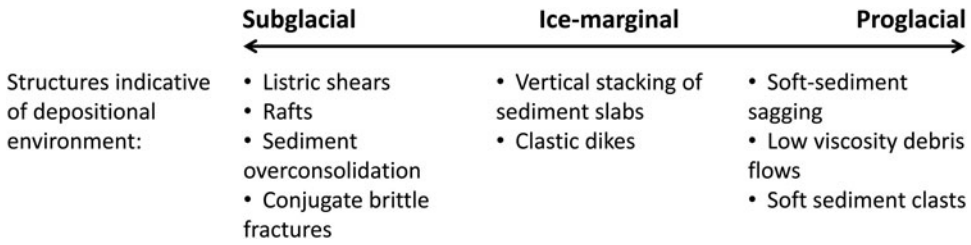


**Fig. 13.** Schematic continuum of deformation structures found in association with particular depositional settings, based on evidence from this study (note, other studies may suggest different depositional contexts).

margin (e.g. Dreimanis and Rappol, 1997; Lee and Phillips, 2008; van der Meer and others, 2009; Rijsdijk and others, 2010) and thus sediments at Barnum Point are considered to be subglacial to proglacial (Table 1). Although commonly recognised, the interpretation of such hydrofractures is strongly influenced by what is seen at the microscale (e.g. Phillips and others, 2007, 2013b), but it is not clear how such observations may correspond to the mesoscale of field analysis (e.g. Dreimanis and Rappol, 1997; Knight, 2015).

Brecciated silt/clay beds and the formation of transported soft-sediment clasts and larger rafts reflect a combination of subglacial shearing (e.g. Point Partridge; Figs 6c and f) and proglacial fluvial transport leading to clast rounding and deposition within the base of channels (Figs 5c and 6b). Soft-sediment clasts have also reported elsewhere in the Puget lowlands proglacial environment (Knight, 2009). Upward-going dewatering structures and associated deformation at Double Bluff (Fig. 12) is typical of upward water injection caused by high-porewater pressure ahead of the ice margin (Knight, 2006; Rijsdijk and other, 2010). Such structures have been termed extrusion moraines and have been noted as proglacial features directed ahead of a low-permeability zone with proglacial permafrost (Knight, 2006).

## Model of Ice–Bed Interactions

Evidence from Whidbey Island and Camano Island reveals more complex interplays between ice, bed and environmental controls such as sediment availability and accommodation space that has been previously recognised from regional sedimentary evidence (e.g. Domack, 1984; Dethier and others, 1995; Demet and others, 2019). This study also highlights that well-sorted proglacial sediments, in particular deposited in outwash settings, can be interrupted by episodic mass/debris flows (West Beach, Barnum Point and Ebey Lodge) or sheet gravels (Ebey Lodge and Double Bluff). This type of depositional setting can be classified as a Salisbury-type delta typical of shallow water and shifting channel environments (Salisbury, 1892) rather than a traditional subaerial outwash sandur. Diamicton beds, reflecting flows of different viscosities, are common in waterlain settings (Talling and others, 2012) but flow depth is commonly unknown and could even be subaerial if sediments are wet and/or fine grained. Evidence from such mass flow sediments within moraines and morainal banks (van der Wateren, 1994; Bennett, 2001) shows that creation of local relief can favour instability and flow activity. The interpretation of morainal banks accumulating in grounding line zones (Demet and others, 2019) is supported by the presence of subaqueous mass flows ahead of the grounding line (Hicock and others, 1981; Dethier and others, 1995; Demet and others, 2019). Evidence of ice–bed interactions by margin oscillation in these locations is shown by brittle fracture and shearing (Barnum Point and Ebey Lodge). However, despite the presence of mass flow deposits, relative sea-level position or its changes over time cannot be evaluated based on this evidence alone.

A significant issue in identifying the depositional setting in which ice–bed interactions take place is that most deformation structures are not unequivocally diagnostic of any one single setting. For example, variations in ice–bed coupling can result in evidence for waterlain deposition even in a subglacial environment (Piotrowski and others, 2006). Studies of subglacial deformation structures also show that these vary over time and space, and the presence of some structures (e.g. dewatering structures indicative of increasing bed strength and viscosity) may in turn make other structures more or less likely to form (e.g. where dewatering reduces the likelihood of folding, or where folding can lead to parasitic clastic dikes) (e.g. Lee and Phillips, 2008). Thus, inferences of depositional setting should be made in a sedimentary sequence context and not based purely on the presence/absence of certain deformation structures. This is particularly the case where the ice margin terminates in water and where, as a result, there is not a clear spatial delimitation between subglacial and proglacial environments (Table 1). In such a setting, ice lift-off from its bed and minor marginal oscillations mean that 'subglacial' signatures can develop ahead of the ice margin and 'proglacial' signatures can develop below the ice bed. Figure 13 lists the typical deformation structures found within sediment sequences attributed to subglacial, ice-marginal and proglacial depositional settings in the Puget Lowlands, based on evidence presented in this study. Also, some structures such as sediment folds can be found in several settings and thus cannot in isolation be considered as diagnostic of a single setting only. It should also be noted that other studies may attribute deformation structures to other depositional environments than those listed in Figure 13.

### Evidence from deformation structures

The presence of both ductile and brittle deformation structures within the same stratigraphic levels (e.g. Point Partridge and Barnum Point) shows that these structures were formed coevally. Thus, deformation should be considered along a continuum between simple shear (ductile) and pure shear (brittle) end-members, depending on clast:matrix ratios, grain size distribution, porewater content and strain history (Phillips and others, 2007; Lee and Phillips, 2013; Knight, 2015). Recent studies show that strain history can be overprinted within sediment stratigraphies at micro- to mesoscales (Phillips and others, 2013b; Phillips and Hughes, 2014). This is clearly seen at the study sites where, for example, clastic dikes parasitically feed from shear planes (Fig. 8c) and fold hinges (Fig. 8f) and where folds are generated by differential movement along shear planes (Fig. 8e). Different deformation structures can therefore be formed in different depositional settings (Fig. 13), and several different types of deformation structures can be observed at each site (Table 2, Fig. 3). In combination, this means it is difficult to unequivocally assign a specific depositional setting to sediment formation at each site (Table 1).

Although sediments and structures reported in this study are interpreted in the context of ice–bed interactions, the Puget

https://doi.org/10.1017/aog.2019.33 Published online by Cambridge University Press

Sound region is seismically active, and late Quaternary and Holocene earthquakes have been reported based on evidence from radiocarbon dating of buried and displaced soils, and on glacigenic sediments that have subsequently been deformed (Johnson and others, 1996, 2004). Ice lobe advance and retreat and repeated loading/unloading cycles can potentially contribute to the triggering of neotectonic activity, as has been reported from around some glacier margins (e.g. Knight, 1999b; Turpeinen and others, 2008; van Loon and Pisarska-Jamroży, 2014). Thus, although the structures presented in this study are stratigraphically confined and a seismogenic origin is not likely, it cannot be wholly excluded, and may have been amplified by glacioisostatic uplift (Thorson, 1989). Booth and others (2004) describe strain rates of about 0.25–1.00 mm $yr^{-1}$ for the last several hundred thousand years in the Puget Lowland, and this may have destabilised deformable glacigenic sediments.

## Conclusions

Glacigenic sediments and sedimentary structures at Camano Island and Whidbey Island, Puget Sound, provide evidence for both ductile deformation and brittle fracture processes during late Wisconsinan advance and retreat and associated with different depositional settings (Fig. 13). Sediments include diamictons with sand and gravel interbeds, and subaqueous massive and cross-bedded sands, gravels and silts with interbedded diamictons that were formed by debris flows. It is suggested that the range of structures present within these sediments (Table 2) attests to different styles of ice–bed interactions that lead to variations in subglacial and proglacial porewater pressure that drive the formation of both ductile and brittle deformational styles. The controls on sediment dynamics discussed in this study have implications for the interpretation of similar sediment successions along other subaqueous ice margins.

**Acknowledgements.** I thank Matteo Spagnolo and an anonymous reviewer for their comments on a previous version of this paper.

## References

**Bennett MR** (2001) The morphology, structural evolution and significance of push moraines. *Earth-Science Reviews* **53**, 197–236.

**Blažauskas N, Jurgaitis A and Šinkūnas P** (2007) Patterns of Late Pleistocene proglacial fluvial sedimentation in the SE Lithuanian Plain. *Sedimentary Geology* **193**, 193–201.

**Booth DB** (1986) Mass balance and sliding velocity of the Puget Lobe of the Cordilleran ice sheet during the last glaciation. *Quaternary Research* **25**, 269–280.

**Booth DB** (1991) Glacier physics of the Puget Lobe, southwest Cordilleran ice sheet. *Géographie Physique et Quaternaire* **45**, 301–315.

**Booth DB** (1994) Glaciofluvial infilling and scour of the Puget Iowland, Washington, during ice-sheet glaciation. *Geology* **22**, 695–698.

**Booth DB, Troost KG and Hagstrum JT** (2004) Deformation of Quaternary strata and its relationship to crustal folds and faults, south-central Puget Lowland, Washington State. *Geology* **32**, 505–508.

**Boulton GS and Caban P** (1995) Groundwater flow beneath ice sheets: Part II – its impact on glacier tectonic structures and moraine formation. *Quaternary Science Reviews* **14**, 563–587.

**Boulton GS and Hindmarsh RCA** (1987) Sediment deformation beneath glaciers: rheology and geological consequences. *Journal of Geophysical Research* **92**(B9), 9059–9082.

**Croot DG** (1987) Glacio-tectonic structures: a mesoscale model of thin-skinned thrust sheets? *Journal of Structural Geology* **9**, 797–808.

**Demet BP, Nittrouer JA, Anderson JB and Simkins LM** (2019) Sedimentary processes and ice sheet grounding-zone wedges revealed by outcrops, Washington State (USA). *Earth Surface Processes and Landforms* **44**, 1209–1220.

**Denis M, Buoncristiani J-F and Guirand M** (2009) Fluid-pressure controlled soft-bed deformation sequence beneath the surging Breiðamerkurjökull (Iceland, Little Ice Age). *Sedimentary Geology* **221**, 71–86.

**Dethier DP, Dragovich JD, Sarna-Wojcicki AM and Fleck RJ** (2008) Pumice in the interglacial Whidbey Formation at Blowers Bluff, central Whidbey Island, WA, USA. *Quaternary International* **178**, 229–237.

**Dethier DP, Pessl Jr F, Keuler RF, Balzarini MA and Pevear DR** (1995) Late Wisconsinan glaciomarine deposits and isostatic rebound, northern Puget Lowland, Washington. *GSA Bulletin* **107**, 1288–1303.

**Domack EW** (1984) Rhythmically bedded glaciomarine sediments on Whidbey Island, Washington. *Journal of Sedimentary Petrol* **54**, 589–602.

**Dreimanis A and Rappol M** (1997) Late Wisconsinan sub-glacial clastic intrusive sheets along Lake Erie bluffs, at Bradtville, Ontario, Canada. *Sedimentary Geology* **111**, 225–248.

**Easterbrook DJ** (1969) Pleistocene chronology of the Puget Lowland and San Juan Islands, Washington. *Geological Society of America Bulletin* **80**, 2273–2286.

**Easterbrook DJ** (1992) Advance and retreat of Cordilleran ice sheets in Washington, USA. *Géographie Physique et Quaternaire* **46**, 51–68.

**Easterbrook DJ** (2003) Cordilleran ice sheet glaciation of the Puget Lowland and Columbia Plateau and alpine glaciation of the North Cascade Range. In Easterbrook DJ (ed.), *Quaternary Geology of the United States, INQUA 2003 Field Guide*. Washington, Reno, NV: DRI, pp. 265–286.

**Eyles N, Eyles CH and Miall AD** (1983) Lithofacies types and vertical profile models; an alternative approach to the description and environmental interpretation of glacial diamict and diamictite sequences. *Sedimentology* **30**, 393–410.

**Fulton RJ** (1991) A conceptual model for growth and decay of the Cordilleran ice sheet. *Géographie Physique et Quaternaire* **45**, 281–286.

**Goldstein B** (1994) Drumlins of the Puget Lowland, Washington State, USA. *Sedimentary Geology* **91**, 299–311.

**Hicock SR and Armstrong JE** (1985) Vashon drift: definition of the formation in the Georgia depression, southwest British Columbia. *Canadian Journal of Earth Sciences* **22**, 748–757.

**Hicock SR, Dreimanis A and Broster BE** (1981) Submarine flow tills at Victoria, British Columbia. *Canadian Journal of Earth Sciences* **18**, 71–80.

**Hindmarsh R** (1997) Deforming beds: viscous and plastic scales of deformation. *Quaternary Science Reviews* **16**, 1039–1056.

**Huntley DH and Broster BE** (1993) Polyphase glacigenic deformation of advance glaciofluvial sediments, near Big Creek, British Columbia. *Géographie Physique et Quaternaire* **47**, 211–219.

**Johnson SY and 5 others** (1996) The southern Whidbey Island fault: an active structure in the Puget Lowland, Washington. *GSA Bulletin* **108**, 334–354.

**Johnson SY and 10 others** (2004) Evidence for late Holocene earthquakes on the Utsalady Point Fault, northern Puget Iowland, Washington. *Bulletin of the Seismological Society of America* **94**, 2299–2316.

**Jopling AV and Walker RG** (1968) Morphology and origin of ripple-drift cross-lamination, with examples from the Pleistocene of Massachusetts. *Journal of Sedimentary Petrology* **38**, 971–984.

**Knight J** (1999a) Morphology and palaeoenvironmental interpretation of deformed soft-sediment clasts: examples from within Late Pleistocene glacial outwash, Tempo Valley, Northern Ireland. *Sedimentary Geology* **128**, 293–306.

**Knight J** (1999b) Geological evidence for neotectonic activity during deglaciation of the southern Sperrin Mountains, Northern Ireland. *Journal of Quaternary Science* **14**, 45–57.

**Knight J** (2006) Geomorphic evidence for active and inactive phases of Late Devensian ice in north-central Ireland. *Geomorphology* **75**, 4–19.

**Knight J** (2009) Significance of soft-sediment clasts in glacial outwash, Puget Sound, USA. *Sedimentary Geology* **220**, 126–133.

**Knight J** (2015) Ductile and brittle styles of subglacial sediment deformation: an example from western Ireland. *Sedimentary Geology* **318**, 85–96.

**Kovanen DJ and Slaymaker O** (2004) Relict shorelines and ice flow patterns of the northern Puget Lowland from lidar data and digital terrain modelling. *Geografiska Annaler* **86A**, 385–400.

**Krzyszkowski D** (1994) Sedimentology of Wartanian outwash near Bełchatów, central Poland. *Boreas* **23**, 149–163.

**Landvik JY and Mangerud J** (1985) A Pleistocene sandur in western Norway: facies relationships and sedimentological characteristics. *Boreas* **14**, 161–174.

**Lee JR and Phillips ER** (2008) Progressive soft sediment deformation within a subglacial shear zone – a hybrid mosaic-pervasive deformation model for

https://doi.org/10.1017/aog.2019.33 Published online by Cambridge University Press

Middle Pleistocene glaciotectonised sediments from eastern England. *Quaternary Science Reviews* **27**, 1350–1362.

**Lee JR and Phillips E** (2013) Glacitectonics – a key approach to examining ice dynamics, substrate rheology and ice-bed coupling. *Proceedings of the Geologists' Association* **124**, 731–737.

**Lowe DR** (1975) Water escape structures in coarse-grained sediments. *Sedimentology* **22**, 157–204.

**Mosher DC and Hewitt AT** (2004) Late quaternary deglaciation and sea-level history of eastern Juan de Fuca Strait, Cascadia. *Quaternary International* **121**, 23–39.

**Mulder T and Alexander J** (2001) The physical character of subaqueous sedimentary density flows and their deposits. *Sedimentology* **48**, 269–299.

**Owen G and Moretti M** (2011) Identifying triggers for liquefaction-induced soft-sediment deformation in sands. *Sedimentary Geology* **235**, 141–147.

**Phillips ER and 6 others** (2018a) Progressive ductile shearing during till accretion within the deforming bed of a palaeo-ice stream. *Quaternary Science Reviews* **193**, 1–23.

**Phillips ER, Evans DJA, van der Meer JJM and Lee JR** (2018b) Microscale evidence of liquefaction and its potential triggers during soft-bed deformation within subglacial traction tills. *Quaternary Science Reviews* **181**, 123–143.

**Phillips E, Everest J and Reeves H** (2013a) Micromorphological evidence for subglacial multiphase sedimentation and deformation during overpressurized fluid flow associated with hydrofracturing. *Boreas* **42**, 395–427.

**Phillips E and Hughes L** (2014) Hydrofracturing in response to the development of an overpressurised subglacial meltwater system during drumlin formation: an example from Anglesey, NW Wales. *Proceedings of the Geologists Association* **125**, 296–311.

**Phillips E, Lipka E and van der Meer JJM** (2013b) Micromorphological evidence of liquefaction, injection and sediment deposition during basal sliding of glaciers. *Quaternary Science Reviews* **81**, 114–137.

**Phillips E, Merritt J, Auton C and Golledge N** (2007) Microstructures in subglacial and proglacial sediments: understanding faults, folds and fabrics, and the influence of water on the style of deformation. *Quaternary Science Reviews* **26**, 1499–1528.

**Piotrowski JA and Kraus AM** (1997) Response of sediment to ice-sheet loading in northwestern Germany: effective stresses and glacier-bed stability. *Journal of Glaciology* **43**, 495–502.

**Piotrowski JA, Larsen NK, Menzies J and Wysota W** (2006) Formation of subglacial till under transient bed conditions: deposition, deformation, and basal decoupling under a Weichselian ice sheet lobe, central Poland. *Sedimentology* **53**, 83–106.

**Pisarska-Jamroży M and Zieliński T** (2014) Pleistocene sandur rhythms, cycles and megacycles: interpretation of depositional scenarios and palaeoenvironmental conditions. *Boreas* **43**, 330–348.

**Porter SC and Swanson TW** (1998) Radiocarbon age constraints on rates of advance and retreat of the Puget Lobe of the Cordilleran ice sheet during the last deglaciation. *Quaternary Research* **50**, 205–213.

**Rijsdijk KF, Warren WP and van der Meer JJM** (2010) The glacial sequence at Killiney, SE Ireland: terrestrial deglaciation and polyphase glacitectonic deformation. *Quaternary Science Reviews* **29**, 696–719.

**Salamon T** (2009) Origin of Pleistocene outwash plains in various topographic settings, southern Poland. *Boreas* **38**, 362–378.

**Salisbury RD** (1892) Overwash plains and valley trains. *Geological Survey: Annual Reports State Geologist* **7**, 96–114.

**Shaw J** (1975) Sedimentary successions in Pleistocene ice-marginal lakes. In Jopling AV and McDonald BC (eds), *Glaciofluvial and Glaciolacustrine Sedimentation*. Tulsa, Oklahoma: SEPM Special Publication 23, pp. 281–303.

**Talling PJ, Masson DG, Sumner EJ and Malgesini G** (2012) Subaqueous sediment density flow: depositional processes and deposit types. *Sedimentology* **59**, 1937–2003.

**Thorson RM** (1980) Ice-sheet glaciation of the Puget Lowland, Washington, during the Vashon Stade (Late Pleistocene). *Quaternary Reviews* **13**, 303–321.

**Thorson RM** (1989) Glacio-isostatic response of the Puget Sound area, Washington. *Geological Society of America Bulletin* **101**, 1163–1174.

**Turpeinen H, Hampel A, Karow T and Maniatis G** (2008) Effect of ice sheet growth and melting on the slip evolution of thrust faults. *Earth and Planetary Science Letters* **269**, 230–241.

**van der Meer JJM, Kjaer KH, Krüger J, Rabassa J and Kilfeather AA** (2009) Under pressure: clastic dykes in glacial settings. *Quaternary Science Reviews* **28**, 708–720.

**van der Wateren FM** (1994) Proglacial subaquatic outwash fan and delta sediments in push moraines – indicators of subglacial meltwater activity. *Sedimentary Geology* **91**, 145–172.

**van Loon AJ and Pisarska-Jamroży M** (2014) Sedimentological evidence of Pleistocene earthquakes in NW Poland induced by glacio-isostatic rebound. *Sedimentary Geology* **300**, 1–10.

https://doi.org/10.1017/aog.2019.33 Published online by Cambridge University Press